



**An exploration of the spatial scale over which orientation-dependent surround effects affect contour detection**

Journal:	<i>Journal of Vision</i>
Manuscript ID:	JOV-02287-2010.R1
Manuscript Type:	Original Article
Date Submitted by the Author:	05-Mar-2011
Complete List of Authors:	Schumacher, Jennifer; University of Minnesota, Graduate Program in Neuroscience Quinn, Christina; University of Minnesota, Psychology Olman, Cheryl; University of Minnesota, Psychology; University of Minnesota, Radiology
Key Words/Topics:	psychophysics, contour detection, surround suppression, contour integration, contextual modulation
Special Issue:	

SCHOLARONE™  
Manuscripts

1  
2  
3  
4  
5  
6  
7  
8  
9  
10  
11  
12  
13  
14  
15  
16  
17  
18  
19  
20  
21  
22  
23  
24  
25  
26  
27  
28  
29  
30  
31  
32  
33  
34  
35  
36  
37  
38  
39  
40  
41  
42  
43  
44  
45  
46  
47  
48  
49  
50  
51  
52  
53  
54  
55  
56  
57  
58  
59  
60

**Title:** An exploration of the spatial scale over which orientation-dependent surround effects affect contour detection

**Authors & Affiliations:**  
Jennifer F. Schumacher<sup>1†</sup>, Christina F. Quinn<sup>2</sup>, Cheryl A. Olman<sup>2,3</sup>  
<sup>1</sup>Graduate Program in Neuroscience, University of Minnesota  
<sup>2</sup>Department of Psychology, University of Minnesota  
<sup>3</sup>Department of Radiology, University of Minnesota

**Corresponding Author:**  
Jennifer F. Schumacher  
N218 Elliott Hall  
75 East River Road  
Minneapolis, MN 55455  
Fax: 612-626-2079  
Phone: 612-626-8471  
Email: [schum204@umn.edu](mailto:schum204@umn.edu)  
† Current Address:  
3M Center  
0235-03-F-08  
St. Paul, MN 55144-1000  
Phone: 651-733-8989  
Email: [jfschumacher@mmm.com](mailto:jfschumacher@mmm.com)

**Number of figures and tables:** 6 figures

**Keywords:** psychophysics, contour detection, contour integration, surround suppression, contextual modulation

## Abstract

Contour detection is a crucial component of visual processing; however, performance on contour detection tasks can vary depending on the context of the visual scene. Dakin and Baruch, 2009 showed that detection of a contour in an array of distracting elements depends on the orientation of flanking elements. Here, using a line of five collinear Gabor elements in a field of distractor Gabor elements, we systematically measured the effects of eccentricity, spacing, and spatial frequency on contour detection performance in three different contexts: randomly oriented distractors (control condition), flanking distractors aligned approximately parallel to the target contour (on either side of the collinear Gabors), and flanking orthogonal distractors. In the control condition, contour detection performance was best for larger Gabors (2 cpd) spaced farther apart ( $1.2^\circ$ ). Parallel flankers reduced performance for intermediate and large spacings and sizes compared to the control condition, while orthogonal flankers increased performance for the smallest spacing and size compared to the control condition. The results are fit by a model in which collinear facilitation, which is size-dependent but can persist for several degrees of visual angle, competes with orientation-dependent suppression from the flanking context when elements are separated by less than a degree of visual angle.

**Introduction**

Local image context, or the image features that surround the feature of interest, is an important factor that can either help or hinder one’s performance in a visual task. Contour detection, in particular, is a task that is strongly dependent on the stimulus geometry and the spatial configuration of the visual scene (Bonneh and Sagi, 1998). In a contour detection task, Dakin and Baruch (2009) found that parallel context impaired contour detection performance, while an orthogonal context improved performance. Because both contour integration and orientation-dependent contextual modulation are known to operate over limited spatial scales, the experiment presented here was conducted in order to define the spatial scale over which each mechanism has the strongest effect.

Many studies have investigated possible neural mechanisms serving contour integration and detection in primary visual cortex (V1). One mechanism that might contribute to contour integration is collinear facilitation: both detection thresholds and contrast discrimination thresholds are decreased for collinear elements (Polat, 1999; Cass and Spehar, 2005; Cass and Alais, 2006). A likely anatomical correlate for collinear facilitation in V1 involves the intrinsic horizontal connections between similar orientation columns (Rockland, Lund, et al., 1982; Gilbert and Wiesel, 1989; Malach, Amir, et al., 1993; Bosking, Zhang, et al., 1997). However, several lines of evidence indicate that contour integration relies on more than just collinear facilitation. For example, collinear facilitation occurs in more limited conditions than contour integration (Williams & Hess, 1998; Huang, et al., 2006): while collinearity is important for correct and quick contour detection, about 20° of “jitter”, or the amount of angular deviation from the contour axis, greatly impedes collinear facilitation, but not contour detection (Williams & Hess, 1998). Other differences include: collinear facilitation and contour detection are differentially affected by dichoptic presentation (Huang, Hess, et al., 2006) and contours made of parallel elements (“ladders”) can be as salient as contours made of collinear elements (“snakes”) (Bex, Simmers, et al., 2001). Therefore, while collinear facilitation can be effectively modeled as a mechanism originating in striate cortex, models describing observers’ performance on contour detection tasks generally rely

mechanisms with larger receptive fields (and 2<sup>nd</sup> order contrast such as orientation contrast) (Field, Hayes et al., 1993; May & Hess, 2008; Dakin & Baruch, 2009), which are generally attributed to extrastriate cortical areas.

Another well-characterized visual context effect is orientation-dependent surround suppression: the response to a single element or to collinear Gabor elements is often suppressed by a parallel surround but not by an orthogonal surround (or, the orthogonal surround suppresses more weakly than a parallel surround or the orthogonal surround provides a release from suppression) (Knierim and van Essen, 1992; Nothdurft, Gallant, et al., 1999; Solomon and Morgan, 2000; Zenger-Landolt and Koch, 2001; Dakin and Baruch, 2009). While intrinsic connections in V1 extend only about 2-4 mm on cortex (Blasdel, Lund, et al., 1985; Angelucci, Levitt, et al., 2002; Hupe, Bullier & Lund, 2002; Amir, Harel & Malach, 1993; Grinvald, Lieke, Frostig & Hildesheim, 1994), orientation-dependent surround effects can originate from context separated by 6-9 mm on cortex (Angelucci, Levitt, et al., 2002). As for contour integration, this large spatial scale suggests an extrastriate origin for orientation-dependent surround effects, although this is an open area of research. Whether the cortical mechanisms are striate or extrastriate, the fact that both orientation-dependent surround suppression and contour integration depend strongly on eccentricity, spacing, spatial frequency, and stimulus contrast between the elements (Angelucci, Levitt, et al., 2002; Shani and Sagi, 2005; Dakin and Baruch, 2009) suggests that both of these contextual effects are mediated by relatively low-level visual mechanisms in retinotopic visual cortex.

For the present study, contour detection within a field of randomly oriented distractors provided a baseline against which orientation-dependent surround effects on contour detection could be measured. Our investigation of contour detection with orientation-dependent surround effects was designed to systematically characterize contour detection performance for a range of Gabor element spacings, sizes, and eccentricities to reveal the balance of contour integration and orientation-dependent suppression for visual elements separated by 0.6°-1.6° of visual angle.

## Methods and Materials

*Subjects*

Data were collected from seven subjects (four female, age 21 – 37, mean age 26.9) with normal or corrected to normal vision. The experimental protocols were approved by the Institutional Review Board at the University of Minnesota. Subjects provided written informed consent before participating in the experiments.

*Stimuli*

Stimuli were generated and presented with Matlab (Mathworks, Inc., Natick, MA) and Psychtoolbox (Brainard 1997; Pelli 1997) and an iMac computer with OS X served as the processor. Stimuli were displayed on a NEC 2180UX LCD monitor, subtending 18.7 x 24.5 degrees of visual angle at a viewing distance of 100 cm. The screen luminance was measured with a photometer (Minolta CS-100, Konica-Minolta Corporation, Ramsey, NY, USA) to perform Gamma calibration and obtain a linear brightness response on this monitor.

The stimuli consisted of a constant-size field of Gabor patches (total angular subtent: 11.7°) composed of a rectangular grid of distractor elements, the number of which varied as the spacing between the Gabors changed. Each Gabor patch consisted of a sinusoidal grating (2, 3.3, or 4 cpd) modulated by a Gaussian envelope that varied with spatial frequency ( $\sigma = 0.33/\text{spatial frequency}$ ). Gabors were always presented at 80% contrast on a mean gray background. Phase was randomized, as previous work has shown phase polarity does not affect contour integration in the fovea or near periphery (Hess and Field, 1999). A white square at the center of the field served as the fixation mark.

The target contour was a vertical line of five Gabors (“collinear Gabors”), which could occur either to the left or to the right of fixation on a given trial. For each trial the orientation of the collinear Gabors was randomly selected to be one of six levels of orientation jitter, ranging from 0 to  $\pm\pi/4$  radians. For all conditions the orientations of the distractor elements were drawn from a uniform distribution  $[0, \pi]$ , but relative orientation of neighboring distractors was controlled to avoid collinearities (i.e., orientation for a given element was re-drawn from the distribution if  $\Delta\theta < \pi/6$  when compared against 4 neighbors,

one in each cardinal direction). For the control condition the orientation of the elements on either side of the collinear Gabors was drawn from the same distribution as the rest of the distractor array. For the “parallel” condition the orientation of the flanking distractor elements was drawn from a distribution of orientations parallel to the target Gabors (uniformly distributed,  $[-\pi/4 \pi/4]$ , where 0 is vertical). For the “orthogonal” condition the orientation of the flanking distractor elements was drawn from a distribution of orientations orthogonal to the target Gabors (uniformly distributed,  $[\pi/4 3\pi/4]$ ). In the parallel and orthogonal conditions, the two flanking lines were present on both sides of the visual field, flanking both possible positions for the target collinear Gabors, on every trial. Three stimulus exemplars are shown in Figure 1.

Seven eccentricities ( $1.2^\circ$ ,  $1.6^\circ$ ,  $1.8^\circ$ ,  $2.4^\circ$ ,  $3^\circ$ ,  $3.2^\circ$ ,  $3.6^\circ$ ), three spacings ( $0.6^\circ$ ,  $0.8^\circ$ ,  $1.2^\circ$ ), and three spatial frequencies (2 cycles per degree (cpd), 3.3 cpd, 4 cpd) defined the parameter space for our stimulus configurations; contour detection performance was measured for eighteen specific combinations from this parameter space. Figure 2 displays several views of the three dimensional parameter space used for these experiments. For each combination of eccentricity, spatial frequency and spacing, performance was measured in three conditions: control, parallel and orthogonal.

### *Psychophysics*

In a two-alternative forced-choice (2AFC) paradigm, subjects responded left or right to indicate where the (jittered) contour appeared. The stimulus was presented for 150 ms on each trial with unlimited time for subjects to respond and a 500 ms pause after the response and before the onset of the next trial. A gray screen was presented during the response period and inter-trial interval. Subjects maintained fixation on the fixation square at the center of the screen; feedback was given by the fixation mark turning green for a correct response and red for an incorrect response. The fixation mark disappeared in between trials.

Tolerance to orientation jitter was measured using the method of constant stimuli. The eccentricity at which the collinear Gabors were presented, the spacing between the Gabor elements, and the spatial frequency of the Gabor patches was constant throughout each block of trials. One block

1  
2  
3 contained 25 trials for each of 6 jitter levels for each of 3 contexts, for a total of 450 trials presented in  
4 random order per block. Each subject completed 2 repetitions of 18 configurations (blocks of trials).  
5  
6  
7 Psychometric functions for each stimulus condition and context (54 total thresholds – 3 contexts for each  
8 of 18 configurations) were estimated from each subject’s performance.  
9  
10  
11  
12  
13

14 *Analysis*

15  
16 Psychometric functions were fit with the Psignifit Matlab toolbox (version 2.5.6, see  
17 <http://bootstrap-software.org/psignifit/>), which is based on Wichmann and Hill, 2001.  
18  
19 Performance over six levels of jitter was fit with a Weibull function using maximum-likelihood  
20 estimation (Figure 3). Thresholds were taken from the 75% correct fitted-point. One subject’s  
21 thresholds were significantly lower than the other six subjects, so this subject was excluded from  
22 further analysis. Thresholds were then averaged over the remaining six subjects per stimulus type  
23 and condition. Additionally, relative suppression indices for the parallel and control conditions  
24 were obtained by subtracting the parallel or control threshold from the orthogonal threshold per  
25 subject, then averaging.  
26  
27  
28  
29  
30  
31  
32  
33  
34  
35  
36

37 Equation 1 shows the general form of a family of models that was tested to describe the contour  
38 integration and orientation-dependent surround effects we observed:  $T$  is the measured threshold,  $T_0$  is a  
39 baseline constant,  $F$  is a function describing facilitation due to collinearity, and  $M$  is a function describing  
40 the strength of the surround effects.  
41  
42  
43  
44  
45  
46

47 
$$T = T_0 + F - M$$
 [1]  
48

49 The  $F$  and  $M$  terms are not physiologically plausible for separations less than the receptive field size,  
50 otherwise (particularly in the case of  $M$ ) the equation would describe self-facilitation and self-masking.  
51  
52 This model is therefore conceptualized as addressing only facilitation and masking arising outside a  
53 neuron’s receptive field; correspondingly, data with spacing  $< 0.6^\circ$  were not fit.  
54  
55  
56  
57  
58  
59  
60



Several functional forms were tested for both F and M, using either exponential or Gaussian shapes as a function of either spacing (degrees) or spacing normalized by element size ( $\text{spc}_{\text{rel}}$ , in units of  $\lambda$ ). All models had six free parameters; the best fit (measured by sum of squared errors) was obtained with the following functional form:

$$T = T_0 + c_f e^{-\frac{\text{spc}_{\text{rel}}^2}{2\sigma_f^2}} + c_m e^{-\frac{\text{spc}}{\Delta_m}} \quad [2]$$

$$\text{with } \Delta_m = c_1 + c_2 \cos^2(\theta_{\text{rel}}) \quad [3]$$

In [2], the spatial scale,  $\Delta_m$ , of the masking term depends on the average orientation of the flankers relative to the target contour ( $0$ ,  $\pi/4$ , or  $\pi/2$ ), but also has an orientation-independent term ( $c_1$ ). Models in which  $\cos^2(\theta_{\text{rel}})$  modulated the amplitude, rather than the spatial extent, of the surround-effects term were also tested but did not fit the data as well as the model presented above.

## Results

We measured human subjects' performance for contour detection in three contexts (control, parallel, and orthogonal – referring to the orientation of the distractor Gabor elements immediately adjacent to the target contour) at eighteen different stimulus configurations differing in eccentricity, spacing, and spatial frequency. The degree of jitter at which a subject could no longer distinguish the target contour from a line of randomly oriented Gabor elements (75% accuracy) was used to evaluate the subjects' threshold (tolerance for orientation jitter) in a contour detection task.

The control condition should best match results from previous contour detection research with randomly oriented distractors. Performance was better for 0.8° separation than for 0.6° separation (dashed line versus solid line) but in all cases decreased as eccentricity increased (Figure 4A). No difference in performance was seen across spatial frequency (Figure 4C), consistent with previous work (Dakin and Hess, 1998). However, in contradiction to previous reports (Hess and Dakin, 1997), contour detection was not scale invariant: for a fixed eccentricity, performance increased significantly as spacing increased, even though size also increased so that relative spacing was constant (Figure 4D,  $F_{2,15} = 12$ ,  $p = 0.0008$ , ANOVA). The increase in performance was also significant when spacing, spatial frequency, and eccentricity were scaled together (Figure 4E,  $F_{2,30} = 4.85$ ,  $p = 0.015$  across conditions, non-significant results for the interaction and no main effect of eccentricity (solid and dotted lines), 2-way ANOVA).

The orthogonal condition is the condition in which orientation-tuned suppression from the flanking context should be minimized. Indeed, the tolerance to orientation jitter in the orthogonal condition was improved over the control condition for most configurations. Unlike the control condition, performance was relatively consistent across eccentricity when the target contour was flanked by orthogonal distractors (Figure 5A). Performance overall weakly decreased with an increase in spacing and also decreased with an increase in spatial frequency, for a fixed spacing, (Figure 5B-C); the decrease in performance is significant in the case of spatial frequency ( $F_{2,30} = 3.83$ ,  $p = 0.033$  across spatial frequency,

non-significant results for the interaction and no main effect of eccentricity (solid and dotted lines), 2-way ANOVA, Figure 5C).

Finally, the parallel condition is the condition in which any iso-orientation suppression effects should be largest. Performance during the parallel condition was always worse than performance on the orthogonal or control conditions. Data from the parallel condition are shown in Figure 6, along with data from the control condition, in the form of suppression indices calculated relative to the performance on the orthogonal task. The greatest effect of orientation-dependent suppression is seen at the closest spacings and lowest spatial frequencies (largest sizes, Figure 6B-C).

The observed pattern of results at 2.4 degrees eccentricity was fit by a combination of contour integration and orientation-dependent surround effects to predict observers' contour detection thresholds as a function of element size and spacing, and flanker orientation. Measured thresholds for seven stimulus configurations (21 conditions) are shown in Figure 7 along with thresholds predicted by the model. While none of the models tested (see Methods) provided a perfect fit to the data, this model succeeds in approximating the observed interaction between relative spacing and flanker orientation (bottom right, Figure 7B): thresholds for the control condition are closer to the parallel condition for close spacings, but closer to the orthogonal condition for the largest spacing. This z-shaped pattern describes a system in which orientation-dependent surround effects dominate at close spatial scales but persist only for the parallel context when elements are separated by  $0.8^\circ$  or more. The characteristic space constant ( $\Delta_m$ ) in the parallel condition at  $2.4^\circ$  eccentricity was  $0.65^\circ$ , which corresponds to approximately 4-5 mm across the cortical surface in V1, assuming typical human cortical magnification (Engel, Glover et al., 1997). This spatial scale is consistent with other observations of orientation-dependent surround suppression (Angelucci, Levitt et al. 2002), but on the high end of values typically reported for intrinsic inhibitory connections in V1. The modeled  $\sigma_f$  for the collinear facilitation term was even larger:  $3.4\lambda$ , therefore ranging from  $0.9^\circ$  to  $1.8^\circ$ , which at  $2.4^\circ$  would span 6-12 mm in V1.

**Discussion**

This systematic study of contour detection performance as a function of element size, spacing, and flanking context extends our understanding of the interplay between contour integration and orientation-dependent suppressive surround effects. In the control condition, our data are largely consistent with previous reports: performance was consistent over the range of 2-4 cpd (Dakin and Hess, 1998; May & Hess, 2008) and decreased with increasing eccentricity. Our results differ from previous reports in that contour detection performance was not scale invariant, but as discussed below, this is likely due to the relatively small element separation used in these experiments. We have also replicated the orientation-dependent flanker effects from Dakin and Baruch, 2009. However, our results extend previous work to show that the size and spacing of the Gabor elements determines whether orthogonal flankers will confer a detection advantage or parallel flankers will impair performance. A simple computational model interpreting these data suggests that performance is determined by a balance of contour integration with orientation-dependent surround effects as spacing and spatial frequency interact.

The orthogonal condition minimizes orientation-dependent flanker effects, thus serving as a baseline for estimating contour integration performance as it depends on element spacing. In keeping with previous models of contour integration as a mechanism that operates at a relatively coarse spatial scale (Field, Hayes et al., 1993; Mundhenk & Itti, 2005; May & Hess, 2008; Dakin & Baruch, 2009), performance in the orthogonal condition generally depended weakly on element spacing and was the best for the largest Gabor elements. An interesting finding is the size-dependence of performance on the contour detection task that is evident for the orthogonal condition (Fig. 5C) but absent for the control condition and largely absent in previously published literature. One possible interpretation of this finding is that the orthogonal context unmasks size-dependence in the contour integration mechanism (which should be present at a fixed spacing if the mechanism scales with relative spacing, as modeled in this and previous work). According to this interpretation, the size-dependence would not be evident in the control condition because, even though relative spacing is increasing with element size, larger elements are also

providing greater orientation-dependent suppression at the smaller relative spacings. However, our data for the parallel condition do not support this interpretation: performance is consistently poor for all sizes, which indicates strong orientation-dependent effects for all sizes, not just the larger size. . Because of the data from the parallel conditions, models with size-dependent terms (see Methods) for the orientation-dependent suppression, which might have produced size-independence in the control condition, did an inferior job of fitting the overall pattern of results. Therefore our model, which relies on a size-independent term for the orientation-dependent suppression, fails to capture the lack of size-dependence in the control condition (Fig. 7B, lower left panel) and we are unable at this point to provide a good mechanistic explanation for the novel finding of size-dependence in the orthogonal condition.

The control condition can be viewed as intermediate between orthogonal and parallel conditions – the average orientation of the flanking context is  $\pi/4$ , relative to the contour elements. Consistent with this view, performance in the control condition was always bounded by performance on the parallel and orthogonal conditions. The orientation-dependent surround effects that reduced performance on the control and parallel conditions (relative to the orthogonal condition) depended strongly on the spacing and spatial frequency of the elements, decreasing both with increased separation between the individual elements and with decreased size (Fig. 6B, C). Both increased separation and decreased size result in an increased cortical distance between the elements, suggesting that orientation-dependent surround effects depend critically on the distance between cortical representations of stimuli. The dependence on eccentricity, in which the orthogonal condition showed no effect of eccentricity while performance on the normal and parallel conditions decreased as the contour was placed further in the periphery (Fig. 6A), is also consistent with a mechanism that operates over a limited cortical scale and spans a larger angular subtent as cortical magnification decreases.

One way in which these experiments fail to replicate results from the literature is that we observe a lack of scale invariance in the control condition (Fig. 4C). In previous studies, performance has remained consistent as elements were increased in size and the spacing was correspondingly scaled (Hess and Dakin, 1997). This scale invariance should persist to  $4^\circ$  of eccentricity, beyond which the differences

1  
2  
3 between foveal and peripheral performance have been attributed to differences in spatial attention (Hess  
4 and Dakin, 1997; Field, Hayes, et al., 1993; Ito and Gilbert, 1999; Shani and Sagi, 1999). In our study,  
5 performance approached scale invariance in the orthogonal condition when eccentricity was also  
6 increased to match the scaling of size and spacing (Fig. 5E), but not in the control or parallel condition.  
7  
8 The fact that we observed scale invariance in the orthogonal condition, in which orientation-dependent  
9 suppressive effects from the flanking context are minimized, suggests that our data on the control and  
10 parallel conditions might diverge from the published literature because the average spacing between the  
11 elements was smaller than in previous experiments. Indeed, Hess and Dakin, 1997 used a spacing of  
12 about  $4\lambda$  when they reported scale invariance; we only tested scale invariance for relative spacings near  
13  $2.4\lambda$ , and the smaller relative spacing likely increases the importance of suppressive surround effects.

14  
15 An important difference between our design and many contour detection tasks reported in the  
16 literature is that our task is not a search task. While we held the total stimulus subtent constant, previous  
17 experiments testing for scale invariance fixed the number of distractor elements – and important control  
18 in a search task. To test whether the variability in the number of distractor elements affected our results, 4  
19 subjects completed a follow-up experiment collecting the data from Fig. 6D with number of elements  
20 fixed instead of grid size fixed. The results (Figure 8) are almost identical, indicating that the lack of scale  
21 invariance we measure is not a consequence of the variation in the number of total elements in the image.  
22 Our modeling effort indicates that this lack of scale invariance may be attributable the particular balance  
23 of orientation-dependent suppression and facilitation from contour integration at this range of spacings  
24 and sizes. We also collected data on an additional point at a larger spacing ( $1.6^\circ$ ) and smaller spatial  
25 frequency (1.5 cpd). As spacing increases, the difference between the orthogonal and parallel conditions  
26 continues to decrease, which is consistent with orientation-dependent suppression effects operating over a  
27 more limited spatial range than contour integration effects (performance on the orthogonal condition  
28 remains high as spacing increases).

While other research has shown a decrease in performance with an increase in spacing, our data and model show a weak decrease, if any, for the orthogonal condition (fixed element size: Fig. 7B, upper right panel) and an increase in performance for the parallel condition. May & Hess (2008) found that contour detection performance decreased with increasing spacing when element separations ranged from about  $1^\circ$  to  $3^\circ$ , which are mostly larger than the range of spacings we measured. Field, et al. (1993) used spacings between  $0.25^\circ$  and  $0.9^\circ$ , which overlaps with our spacings of  $0.6^\circ$ - $1.2^\circ$ , and found a decrease in spacing. In that study, however, the spatial frequency was much higher (8cpd), resulting in larger relative spacings ( $2\lambda - 7.2\lambda$ ) than ours ( $1.2\lambda - 4.8\lambda$ ). Therefore, it is likely that the lack of significant dependence on spacing that we measure in the orthogonal condition is a consequence of the low relative spacings we used for the experiment, i.e., we were collecting data in a regime where contour integration mechanisms were competing against short-range inhibitory mechanisms. Correspondingly, the increase in performance with spacing for the parallel condition is interpreted as a release from short-range surround suppression effects.

Interestingly, with visual stimuli quite different from ours, using simple tilted or vertical bars as target elements and distractors, a similar spatial scale for the effect of parallel or orthogonal elements on visual search was found (May & Zhaoping, 2009). A target bar was placed  $1^\circ$ - $4^\circ$  from an axis that was aligned parallel or orthogonal to the target and distractors. Our findings would predict a decrement in performance with the parallel axis up to about  $2.5^\circ$  (Fig. 7A, lower panel), which is what May & Zhaoping (2009) observed. Our findings would also predict no suppressive effect from the orthogonal axis within this spatial range (less than  $4^\circ$ ) and they also saw no suppressive effect in this range with an orthogonal axis.

One tool we used in investigating the balance between contour integration and orientation-dependent suppressive effects was a simple computational model that predicted facilitation from contour integration and inhibition from parallel context as a function of element size and separation. This model did not capture all of the observed behavior – for example, the model under-represents the similarity of the thresholds for the control and parallel conditions with small elements (4 cpd) that are closely spaced

(0.6°, Fig. 7B, lower right panel, although note that the data from the follow-up experiment in Fig. 8B show good agreement with model predictions). The reason that the model fails to fit this pair of points well is that it is also constrained to fit the data at 0.8° spacing, 4 cpd elements, where performance on the control condition was almost identical to performance on the *orthogonal* condition. We tried several other types of models, including full image models (multiple orientation and spatial frequency channels) similar to those shown in Dakin & Baruch (2009) and May & Hess (2008), but the other models did not do a better job of capturing this aspect of the observed performance. Thus, the estimated spatial scales for orientation-dependent lateral masking and contour integration can only be approximate, as the fit to the data is limited. However, the general ideas captured by the model are informative, and confidence in the conclusions is bolstered where they are supported by previous literature, as discussed above.

Another limitation of our design is that it cannot separately characterize the contributions of collinear facilitation and contour integration. A second experiment with “ladders” as well as “snakes” (Bex, Simmers, et al. 2001) would be required to allow separate characterization of the contribution of collinear facilitation to the contour detection performance we have measured. Thus, we have used the term “contour integration” to describe the facilitative term in our model, intending that this comprises a combination of low-level collinear facilitation and higher-level mechanisms.

The primary finding of this work is that the orientation-dependent suppressive effects that inhibit contour integration appear to operate over a more limited spatial range than the facilitative mechanisms that serve contour integration. The pattern supporting this conclusion is most evident in Fig. 7B. In the upper right panel, the effect of flanking context is reduced by half when the spacing is doubled, but performance on the contour detection task with orthogonal context (the condition in which flanking effects are minimized) decreases only slightly with the doubling in element spacing. This pattern suggests that, for our set of stimuli in which target elements and distracters are relatively dense, facilitative mechanisms aiding contour integration depend weakly on spacing while orientation-dependent suppressive mechanisms depend more strongly on spacing.



## Conclusion

Contour integration and orientation-dependent flanker effects appear to operate on different spatial scales. In keeping with previous work on local contextual modulation in V1, we find that the spatial scale over which orientation-dependent lateral masking affects contour integration is potentially larger than can be supported by V1-intrinsic mechanisms. The still-longer range of contour integration supports an extrastriate mechanism serving contour integration. The interplay between these two mechanisms indicates that previous findings such as scale invariance in contour detection performance will hold only over a particular range of element spacings, and that observers' ability to detect contours in crowded environments is strongly dependent on local image context.

1  
2  
3  
4  
5  
6  
7  
8  
9  
10  
11  
12  
13  
14  
15  
16  
17  
18  
19  
20  
21  
22  
23  
24  
25  
26  
27  
28  
29  
30  
31  
32  
33  
34  
35  
36  
37  
38  
39  
40  
41  
42  
43  
44  
45  
46  
47  
48  
49  
50  
51  
52  
53  
54  
55  
56  
57  
58  
59  
60

Tables

Table 1. Parameters for model (Eq. 2 & 3) to fit the data as shown in Fig. 7

Parameter:	$T_0$	$c_f$	$\sigma_f$	$c_m$	$c_1$	$c_2$
Value:	26	8.3	3.4	-29	0.19	0.46

For Peer Review

## References

- Angelucci, A., J. B. Levitt, et al. (2002). "Circuits for local and global signal integration in primary visual cortex." Journal of Neuroscience **22**(19): 8633-8646.
- Bex, P. J., Simmers, A. J. and Dakin, S. C. (2001). "Snakes and Ladders: The Contribution of Temporal Modulation to Visual Contour Integration," Vision Research, **41**(27): 3775-378
- Blasdel, G. G., J. S. Lund, et al. (1985). "Intrinsic connections of macaque striate cortex: axonal projections of cells outside lamina 4C." J Neurosci **5**(12): 3350-69.
- Bonneh, Y. and D. Sagi (1998). "Effects of spatial configuration on contrast detection." Vision Res **38**(22): 3541-53.
- Bosking, W. H., Y. Zhang, et al. (1997). "Orientation selectivity and the arrangement of horizontal connections in tree shrew striate cortex." J Neurosci **17**(6): 2112-27.
- Brainard, D. H. (1997). "The psychophysics toolbox." Spatial Vision **10**: 433-436.
- Cass, J. and D. Alais (2006). "The mechanisms of collinear integration." J Vis **6**(9): 915-22.
- Cass, J. R. and B. Spehar (2005). "Dynamics of collinear contrast facilitation are consistent with long-range horizontal striate transmission." Vision Res **45**(21): 2728-39.
- Dakin, S. C. and N. J. Baruch (2009). "Context influences contour integration." J Vis **9**(2): 13 1-13.
- Dakin, S. C. and R. F. Hess (1998). "Spatial-frequency tuning of visual contour integration." J Opt Soc Am A Opt Image Sci Vis **15**(6): 1486-99.
- Engel, S. A., G. H. Glover, et al. (1997). "Retinotopic organization in human visual cortex and the spatial precision of functional MRI." Cerebral Cortex **7**: 181-192.
- Field, D. J., A. Hayes, et al. (1993). "Contour integration by the human visual system: evidence for a local "association field"." Vision Res **33**(2): 173-93.
- Gilbert, C. D. and T. N. Wiesel (1989). "Columnar specificity of intrinsic horizontal and corticocortical connections in cat visual cortex." J Neurosci **9**(7): 2432-42.
- Hess, R. and D. Field (1999). "Integration of contours: new insights." Trends Cogn Sci **3**(12): 480-486.
- Hess, R. F. and S. C. Dakin (1997). "Absence of contour linking in peripheral vision." Nature **390**(6660): 602-4.
- Hess, R. F. and D. J. Field (1995). "Contour integration across depth." Vision Res **35**(12): 1699-711.
- Huang, P.-C., Hess, R.F., Dakin, S.C. (2006). "Flank facilitation and contour integration: different sites." Vision Research **46**: 3699-3706.
- Ito, M. and C. D. Gilbert (1999). "Attention modulates contextual influences in the primary visual cortex of alert monkeys." Neuron **22**(3): 593-604.
- Knierim, J. J. and D. C. van Essen (1992). "Neuronal responses to static texture patterns in area V1 of the alert macaque monkey." J Neurophysiol **67**(4): 961-80.
- Malach, R., Y. Amir, et al. (1993). "Relationship between intrinsic connections and functional architecture revealed by optical imaging and *in vivo* targeted biocytin injections in primate striate cortex." Proceedings of the National Academy of Science (USA) **90**: 10469-10473.
- May, K.A. and L. Zhaoping (2009). "Effects of surrounding frame on visual search for vertical or tilted bars." J Vision **9**(13):20, 1-19.

May, K.A. and R.F. Hess (2008). "Effects of element separation and carrier wavelength on detection of snakes and ladders: Implications for models of contour integration." J Vision **8**(13):4, 1-23.

Mundenk, T.N. and L. Itti (2005). "Computational modeling and exploration of contour integration for visual saliency." Biological Cybernetics **93**:188-212.

Nothdurft, H. C., J. L. Gallant, et al. (1999). "Response modulation by texture surround in primate area V1: correlates of "popout" under anesthesia." Vis Neurosci **16**(1): 15-34.

Nygard, G. E., T. V. Looy, et al. (2009). "The influence of orientation jitter and motion on contour saliency and object identification." Vision Res **49**(20): 2475-84.

Pelli, D. G. (1997). "The VideoToolbox software for visual psychophysics: Transforming numbers into movies." Spatial Vision **10**: 437-442.

Polat, U. (1999). "Functional architecture of long-range perceptual interactions." Spat Vis **12**(2): 143-62.

Rockland, K. S., J. S. Lund, et al. (1982). "Anatomical binding of intrinsic connections in striate cortex of tree shrews (*Tupaia glis*)." J Comp Neurol **209**(1): 41-58.

Shani, R. and D. Sagi (2005). "Eccentricity effects on lateral interactions." Vision Res **45**(15): 2009-24.

Solomon, J. A. and M. J. Morgan (2000). "Facilitation from collinear flanks is cancelled by non-collinear flanks." Vision Res **40**(3): 279-86.

Wichmann, F. A. and N. J. Hill (2001). "The psychometric function: I. Fitting, sampling, and goodness of fit." Percept Psychophys **63**(8): 1293-313.

Williams, C.B. and R.F. Hess (1998). "Relationship between facilitation at threshold and suprathreshold contour integration." J Opt Soc Am A **15**(8): 2046-2051.

Zenger-Landolt, B. and C. Koch (2001). "Flanker effects in peripheral contrast discrimination - psychophysics and modeling." Vision Research **41**: 3663-3675.

Zipser, K., V. A. Lamme, et al. (1996). "Contextual modulation in primary visual cortex." J Neurosci **16**(22): 7376-89.

## FIGURE LEGENDS

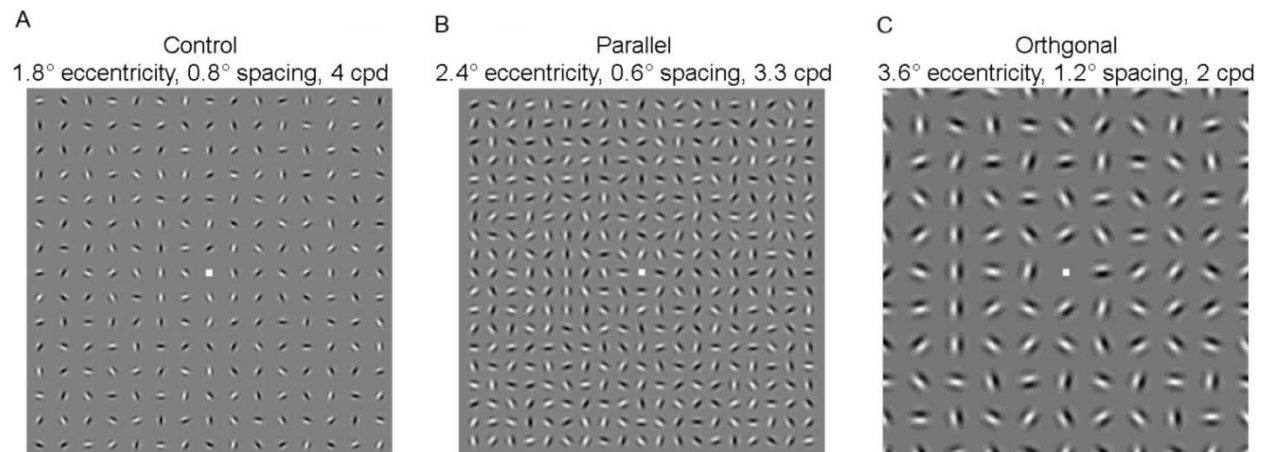


Figure 1: Examples of stimuli with collinear Gabors present on the left side. A) Control condition (randomly oriented flanking distracters): in this example, the target contour is present at 1.6° eccentricity, with 4 cpd Gabors at 0.8° spacing. B) Parallel condition: in this example, the target contour is present at 2.4° eccentricity, with 3.3 cpd Gabors at 0.6° spacing. C) Orthogonal condition: in this example, the target contour is present at 3.6° eccentricity, with 2 cpd Gabors at 1.2° spacing.

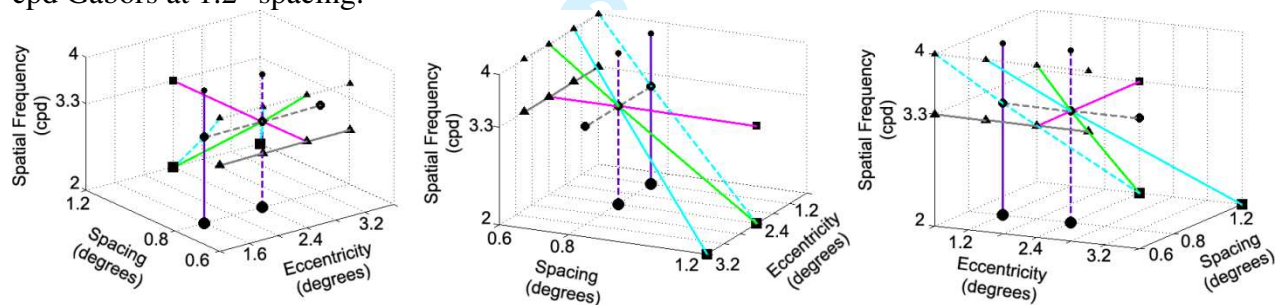


Figure 2: Representation of parameter space covered by these experiments. Color-coded lines indicate comparisons shown in Figures 4-6. Marker shapes indicate spacing (0.6°: triangle, 0.8°: circle, and 1.2°: square); marker sizes indicate spatial frequency (larger markers for lower spatial frequencies). Three views are given to help visualize the three-dimensional space.

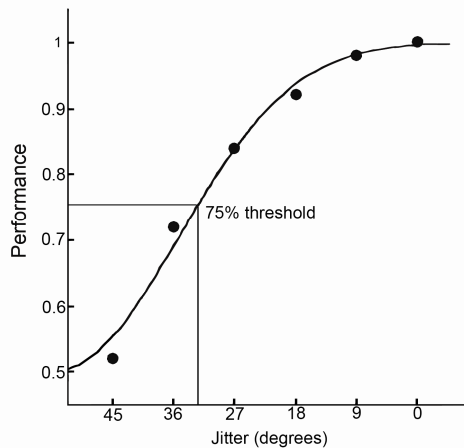


Figure 3: Typical psychometric function (control context, 1.2° eccentricity, 0.6° spacing, 3.3 cpd, subject 1). Percent correct is plotted for six levels of jitter, along with the Weibull function fit to data using maximum-likelihood estimation.

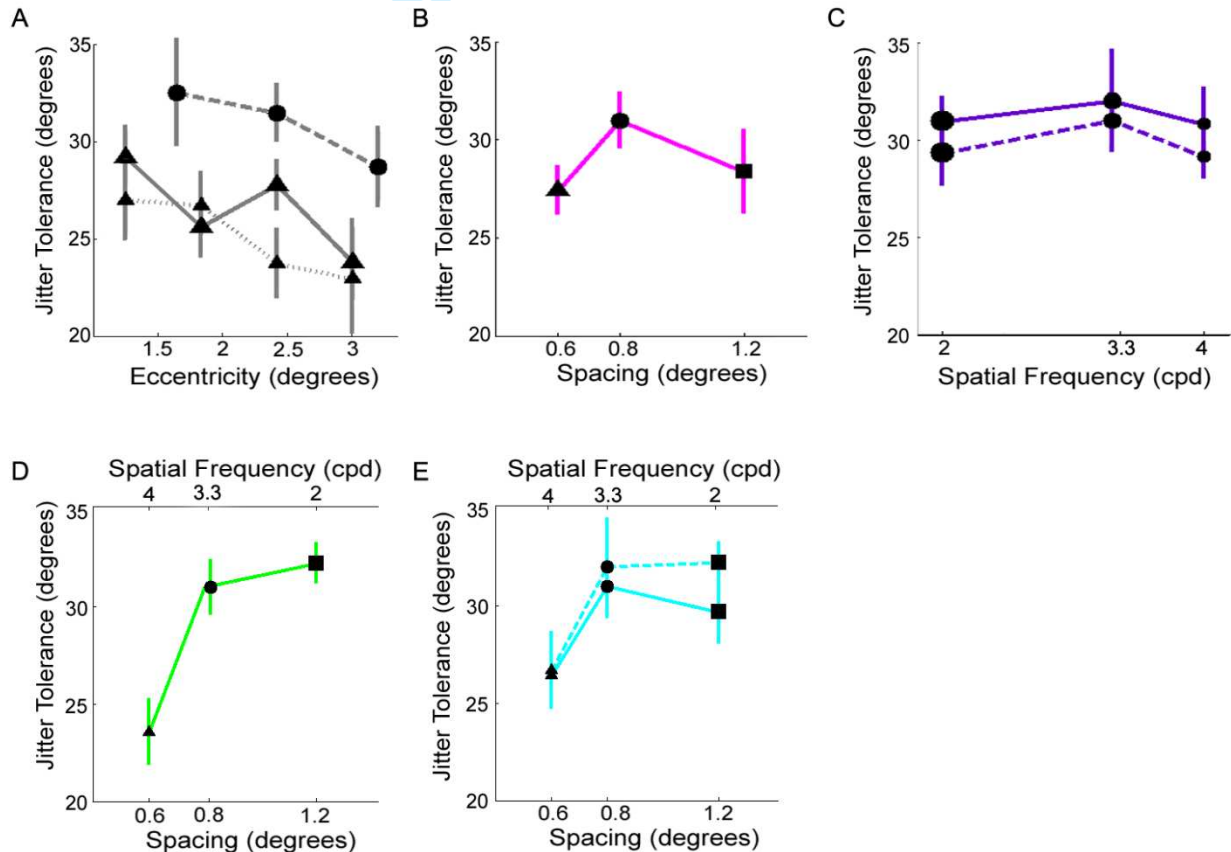


Figure 4: Control condition results. A) Performance as a function of eccentricity. Solid line is 0.6° spacing and 3.3 cpd, dashed line is 0.8° spacing and 3.3 cpd, dotted line is 0.6° spacing and 4 cpd. B) Performance as a function of spacing for 3.3 cpd Gabors at 2.4° eccentricity. C) Performance as a function of element size, for elements spaced at 0.8° with target contours at 1.6° eccentricity (solid line) and 2.4° eccentricity (dashed line). D) At 2.4° eccentricity, performance significantly increased ( $F_{2,15} = 12$ ,  $p = 0.0008$ , ANOVA) as the elements were spaced further apart and were larger in size (relative spacing:  $2.4\lambda$ - $2.6\lambda$ ). E) Performance

improved as elements were moved toward the periphery and scaled according to cortical magnification ( $F_{2,30} = 4.85$ ,  $p = 0.015$ , 2-way ANOVA). The solid line covered eccentricities 1.2°, 1.6°, and 2.4° (relative spacing as in (D)), the dashed line covered eccentricities 1.8°, 2.4°, and 3.6°. Error bars in all panels are SEM,  $n = 6$ .

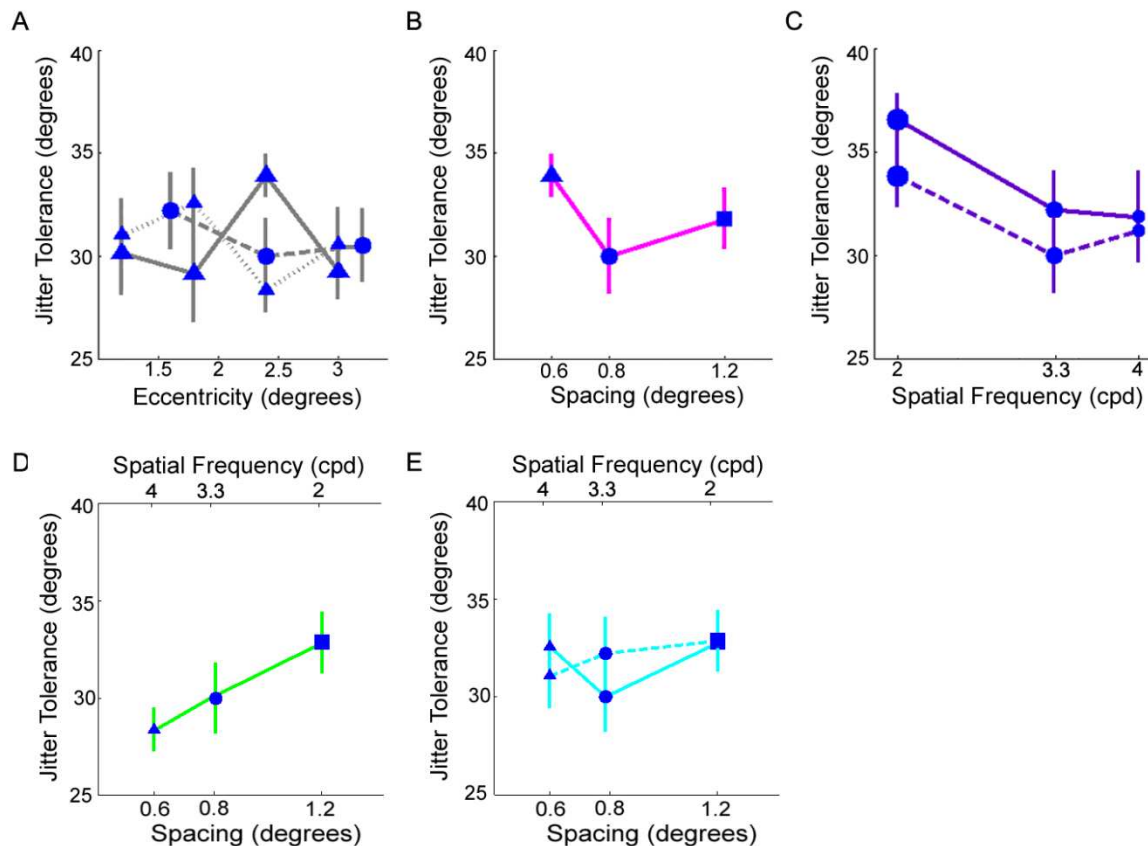


Figure 5: Orthogonal context results. Data are plotted as in Figure 4. The decrease in performance over spatial frequency (C) was statistically significant,  $F_{2,30} = 3.83$ ,  $p = 0.033$ , 2-way ANOVA.



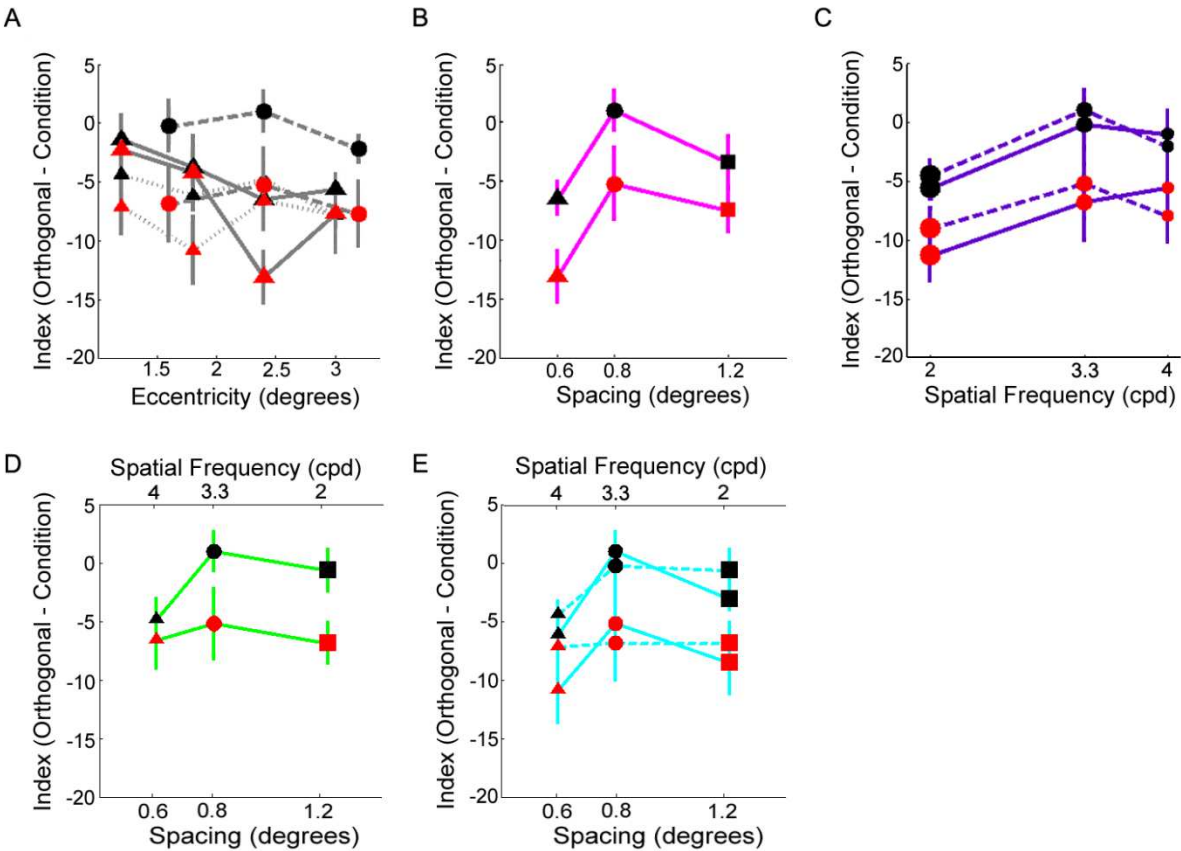


Figure 6: Performance on control and parallel conditions relative to orthogonal condition. Indices were calculated by subtracting thresholds in the control or parallel conditions from the thresholds of the orthogonal condition. Black markers represent the control condition and red markers indicate the parallel condition. Results are grouped as in Figure 4. Suppression indices for the control condition depended significantly on spacing (B), ( $F_{2,15} = 3.73$ ,  $p = 0.049$ , ANOVA) and spatial frequency (C), ( $F_{2,30} = 5.5$ ,  $p = 0.0092$ , 2-way ANOVA). Performance on the control condition also depended significantly on scaling with eccentricity (E), ( $F_{2,30} = 6.51$ ,  $p = 0.0045$ , 2-way ANOVA).



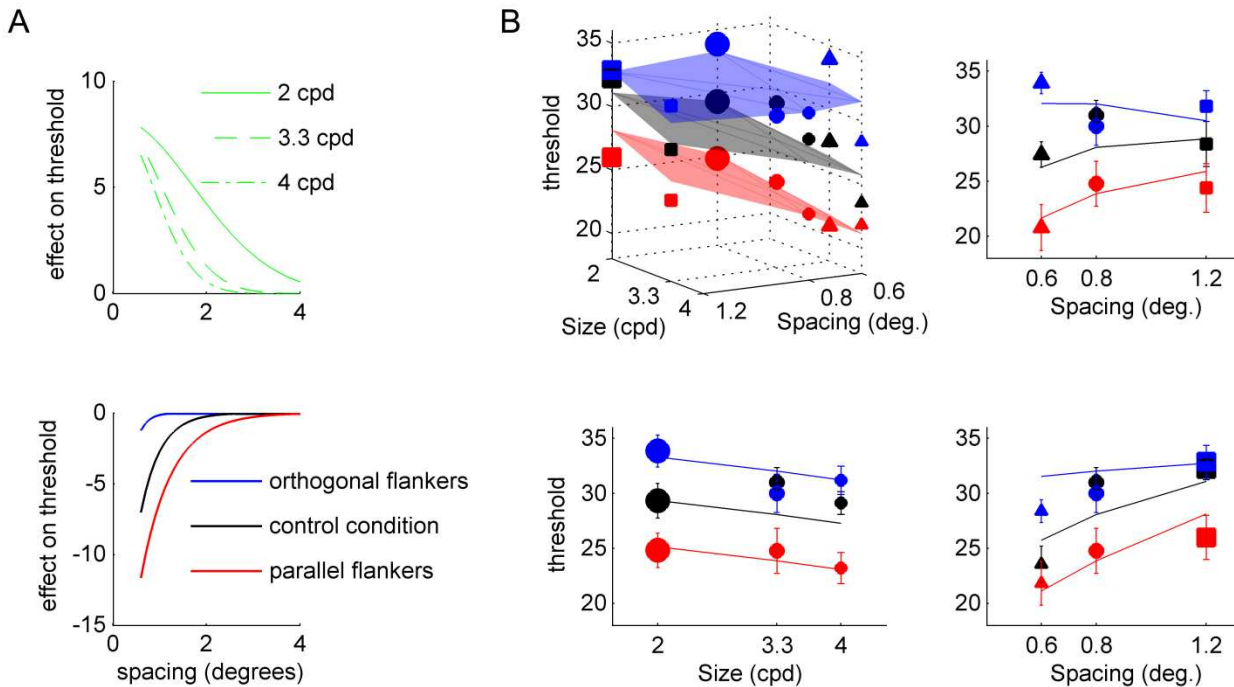


Figure 7: A computational model predicting observer performance as a balance between subtractive orientation-dependent lateral masking and additive size-dependent contour integration terms. A) Model components describing collinear facilitation (green) and orientation-dependent lateral masking (blue: orthogonal flankers; black: control condition; red: parallel flankers) are plotted as a function of element spacing in the visual field. The best fit to the data was obtained modeling collinear facilitation as a function of *relative* spacing, but orientation-dependent suppression as a function of *absolute* spacing. B) The 3D plot in the upper left shows modeled thresholds (shaded surfaces) and measured thresholds (shapes and sizes of data points indicate size and spacing as in Figure 4-6; color indicates flanker orientation) for all conditions at 2.4° eccentricity. The other three panels show slices through this 3D space, with solid lines indicating model fits; error bars on data points are SEM across 6 subjects.

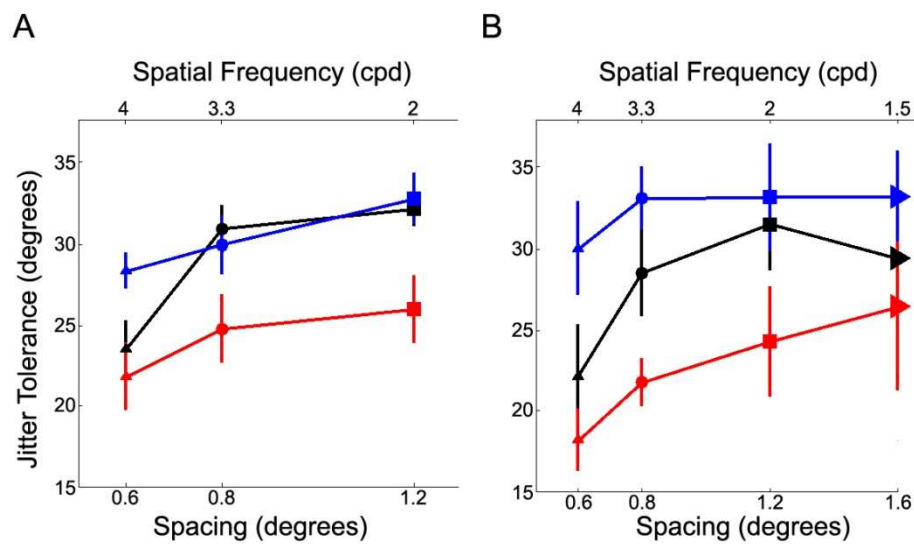


Figure 8: Comparison of results for constant grid size with variable Gabor element number (A) and constant Gabor element number with variable grid size (B). Blue: orthogonal, black: control, red: parallel flankers. Rightward-pointing triangles indicate 1.5 cpd elements separated by 1.6°. Error bars are SEM (n=6 for (A), n=4 for all points in (B) except the condition with 1.6° spacing and 1.5 cpd, for which is n=3 for).